Available online at www.sciencedirect.com
SCIENCE DIRECT®
ELSEVIER
Icarus 167 (2004) 113–128
ICARUS
www.elsevier.com/locate/icarus

The outgassing and composition of Comet 19P/Borrelly from radio observations

Dominique Bockelée-Morvan,[a,*] Nicolas Biver,[a,b] Pierre Colom,[a] Jacques Crovisier,[a] Florence Henry,[a] Alain Lecacheux,[a] John K. Davies,[c] William R.F. Dent,[c] and Harold A. Weaver[d]

[a] *LESIA, Observatoire de Paris, 5 place Jules Janssen, F-92195 Meudon, France*
[b] *ESA-ESTEC SCI-SB, Keplerlaan 1, NL-2200 AG Noordwijk ZH, The Netherlands*
[c] *Astronomy Technology Centre, Royal Observatory, Blackford Hill, Edinburgh, EH93HJ, UK*
[d] *The Johns Hopkins University Applied Physics Laboratory, 11100 Johns Hopkins Road, Laurel, MD 20723-6099, USA*

Received 15 November 2002; revised 18 March 2003

Abstract

Radio spectroscopic observations of Comet 19P/Borrelly were performed during the 1994 apparition and at, and near, the time of the Deep Space 1 flyby in 2001. HCN, CS, CH_3OH, and H_2CO were detected using the 30-m telescope of the Institut de Radioastronomie Millimétrique and the James Clerk Maxwell Telescope, and their production rates relative to water are estimated to be 0.06–0.11, 0.07, 1.7, and 0.4%, respectively. Only upper limits are derived for H_2S and CO. The upper limit for CO/H_2O (< 15%) is not very constraining, while the upper limit for the H_2S/H_2O ratio of 0.45% is near the bottom of the range of values measured for other comets. Observations of the OH radical at the Nançay radio telescope provide water production rates a few weeks before the 1994 and 2001 perihelia. Observations of the 1_{10}–1_{01} water line at 557 GHz with the Odin satellite yield a water production rate of $(2.5 \pm 0.5) \times 10^{28}$ s^{-1} on September 22, 2001, at the time of the Deep Space 1 encounter, and $(3.3 \pm 0.6) \times 10^{28}$ s^{-1} averaged over the September 22–24, 2001 period. The line shapes are asymmetric and blueshifted by $V_0 \sim -0.18$ km s^{-1} for the best observed HCN lines recorded one week after perihelion. The HCN line shapes, and the similar OH and HCN velocity shifts over the September–November 1994 and August–September 2001 periods, favor anisotropic outgassing towards the Sun. Strong outgassing directed along the primary dust jet seen on visible images is not excluded by the HCN line shapes, but unrealistically high gas expansion velocities are required to explain the line shapes in that case.

Keywords: Comets, composition, 19P/Borrelly; Radio observations

1. Introduction

Comet 19P/Borrelly is a Jupiter-family comet having an orbital period of 6.9 yr. Owing to a close approach to Earth at $\Delta = 0.62$ AU only one month after its perihelion on November 1, 1994 at $q = 1.365$ AU, 19P/Borrelly was intensively observed during its 1994 apparition (e.g., Lamy et al., 1998; Cochran and Barker, 1999). Although its 2001 passage (perihelion on September 14) was less favorable for Earth-based observations, many observational campaigns were mounted because 19P/Borrelly was the target of the Deep Space 1 (DS1) mission, a technological mission of the NASA New Millenium Program. DS1, after a flyby of asteroid 9969 Braille in July 1999 (Oberst et al., 2001), encountered 19P/Borrelly on September 22.937, 2001 UT (Soderblom et al., 2002). The optical telescope on DS1 measured the gross physical properties of the nucleus, such as size, shape, spin rate and reflectivity, and revealed a variety of terrains and textures on the surface. Images of the inner dust coma showed several jet-like dust features. Other instrumentation on DS1 included an infrared spectrometer and a plasma experiment.

Relative production rates of the C_2, C_3, CN radicals measured in the coma of 19P/Borrelly near perihelion indicate that this comet is a member of a class that is "depleted" in carbon-chain molecules (A'Hearn et al., 1995; Cochran and Barker, 1999). About half of the Jupiter-family comets belong to this depleted class, possibly because they formed in the Kuiper belt, in contrast to the others, including Oort

* Corresponding author.
E-mail address: dominique.bockelee@obspm.fr (D. Bockelée-Morvan).

0019-1035/$ – see front matter
doi:10.1016/j.icarus.2003.04.001

cloud comets, which may have formed between Uranus and Neptune. A more direct way to investigate compositional differences between Kuiper belt and Oort cloud comets is from observations of *parent* molecules, which sublimate directly from the nucleus. While compositional data are steadily accumulating for Oort cloud comets, measurements of parent molecular abundances in short-period comets are still sparse because they have weaker production rates and are more difficult to observe.

Because of its relatively high gaseous activity near perihelion (water production rate $Q[H_2O] > 10^{28}$ s^{-1}) compared to other Jupiter-family comets, 19P/Borrelly is one of the few opportunities to undertake such measurements with presently available instrumentation. In this paper, we present molecular observations made at radio wavelengths during the 1994 and 2001 passages of 19P/Borrelly. We include:

(1) observations of the 18-cm lines of the OH radical performed at the Nançay radio telescope,
(2) observations at millimeter wavelengths of HCN, CO, H_2CO, CH_3OH, CS, and H_2S using the 30-m telescope of the Institut de Radioastronomie Millimétrique (IRAM),
(3) submillimeter observations of HCN with the James Clerk Maxwell Telescope (JCMT), and
(4) observations of the 1_{10}–1_{01} water line at 557 GHz with the Odin satellite.

Observations were scheduled using IRAM and Odin at the time of the DS1 flyby, in order to characterize the cometary activity during that critical period when DS1 made its closest approach to the nucleus of 19P/Borrelly. Some of the results of these observations were already reported in Bockelée-Morvan et al. (1995, 2002), Biver (1997), Crovisier et al. (2002a), and Lecacheux et al. (2003).

Section 2 presents the observations. Molecular production rates and abundances relative to water are given in Section 3. Section 4 discusses the outgassing pattern from an analysis of the radio line shapes.

2. Observations

2.1. Observations at IRAM 30-m

2.1.1. 1994 passage

The observations at the IRAM 30-m telescope were carried out from November 8.03 to 10.30, 1994 UT, when the heliocentric (r_h) and geocentric (Δ) distances of the comet were 1.37 and 0.68 AU, respectively. The comet was tracked using orbital elements provided a few days before the observations by Brian Marsden from the Central Bureau for Astronomical Telegrams (CBAT). These orbital elements were an improvement over those published in MPC 18259. Comparison of the ephemeris used during our observations to one derived from better post-observation elements shows that pointing offsets due to ephemeris errors were $\sim 3.5''$ towards position angle (PA) $= 90°$. Total pointing errors are estimated to be ~ 4–$5''$, depending on the date. The observations were conducted in beam-switching mode by wobbling the secondary mirror.

The versatility of the IRAM system in 1994 allowed us to use three receivers working at 3, 2, and 1.3 mm wavelength simultaneously. A log of the observations is presented in Table 1. Rotational lines of HCN (J(1–0) at 88.6318 GHz), H_2CO (3_{12}–2_{11} at 225.6978 GHz), and CH_3OH (multiplets at 145 and 157 GHz) were observed. At these frequencies, the half-power beam widths (HPBW) of the 30-m antenna were $26''$ (88 GHz), $16''$ (145 GHz), $15''$ (157 GHz), and $10.6''$ (226 GHz), corresponding to projected radii at the comet between 2600 and 6500 km. The high resolution backends were comprised of a 256-channel filterbank at 100 kHz resolution, and a flexible autocorrelator set in a configuration providing spectral resolutions of 20 and 39 kHz. A splittable 1024-channel filterbank with 1 MHz resolution was connected to the 1.3 and 2 mm receivers.

All three species were detected with signal-to-noise ratios varying from 3.6 (H_2CO) to 7.4 (HCN), although the H_2CO detection is admittedly marginal. Spectra of HCN and CH_3OH are shown in Figs. 1 and 2, respectively. Line areas, in units of main beam brightness temperature (T_{mB}), and line velocity shifts V_0 with respect to the cometary rest velocity, are given in Table 2. The HCN J(1–0) spectrum, and the methanol spectrum obtained by averaging the different lines of the 145 GHz multiplet, show blueshifted lines with $V_0 \sim -0.3$ km s^{-1} with respect to the rest velocity of the nucleus. The HCN J(4–3) line observed on November 9 at JCMT and the OH lines recorded one month earlier (notwithstanding their lower signal-to-noise ratio), are consistent with a similar velocity shift ($V_0 \sim -0.2$ km s^{-1}, Tables 2 and 5).

2.1.2. 2001 passage

During the 2001 passage, observations at IRAM were scheduled from September 19.3 to 24.3, 2001 UT, when the comet had $r_h = 1.36$ AU and $\Delta = 1.48$ AU. Bad weather prevented observations on September 22 and 23, at the exact time of the DS1 flyby. The comet was tracked using orbital elements kindly provided by Daniel Green of CBAT, and the pointing jitter was $\sim 1.5''$ (rms).

The observations were very similar to those performed in 1994, except that four receivers could now be used at the same time. In addition to the 3, 2, and 1 mm receivers, a receiver tunable to frequencies higher than 245 GHz was used. This allowed us to observe the J(3–2) line of HCN at 265.886 GHz. The HCN J(1–0) line was observed in parallel on September 19 to 21. Daily results for HCN are presented in Table 3. HCN was clearly detected on September 20, 21, and 24. Average spectra are displayed in Fig. 1. The CS radical was marginally detected from its J(3–2) and J(5–4) lines at 146.9690 and 244.9356 GHz, respectively (Fig. 3). The observations of H_2S (1_{10}–1_{01} at 168.7624 GHz), H_2CO (225 GHz line), and CO (J(2–1) at

Table 1
Log of IRAM and JCMT observations

Date (UT)	r_h (AU)	Δ (AU)	Molecule	Line	ν (GHz)	$t_{\rm int}$[a] (min)	Spectrometer[b]
IRAM 1994 passage							
1994 November 8.03–8.36	1.367	0.688	HCN	J(1–0)	88.6318	250	100 kHz, 20 kHz
			H_2CO	3_{12}–2_{11}	225.6978	250	100 kHz, 1 MHz, 39 kHz
			CH_3OH	3_0–2_0 E	145.0938	250	1 MHz, 39 kHz
			CH_3OH	3_{-1}–2_{-1} E	145.0974	250	1 MHz, 39 kHz
			CH_3OH	3_0–2_0 A	145.1032	250	1 MHz, 39 kHz
			CH_3OH	3_2–2_2 A^-	145.1243	250	1 MHz, 39 kHz
			CH_3OH	$3_{\pm2}$–$2_{\pm2}$ E	145.1263	250	1 MHz, 39 kHz
			CH_3OH	3_1–2_1 E	145.1319	250	1 MHz, 39 kHz
			CH_3OH	3_2–2_2 A^+	145.1334	250	1 MHz, 39 kHz
1994 November 9.03–9.13	1.368	0.683	HCN	J(1–0)	88.6318	96	100 kHz, 20 kHz
			H_2CO	3_{12}–2_{11}	225.6978	96	100 kHz, 1 MHz, 39 kHz
			CH_3OH	6_0–6_{-1} E	157.0486	96	1 MHz, 39 kHz
			CH_3OH	5_0–5_{-1} E	157.1790	96	1 MHz, 39 kHz
			CH_3OH	4_0–4_{-1} E	157.2460	96	1 MHz, 39 kHz
			CH_3OH	1_0–1_{-1} E	157.2708	96	1 MHz, 39 kHz
			CH_3OH	3_0–3_{-1} E	157.2723	96	1 MHz, 39 kHz
			CH_3OH	2_0–2_{-1} E	157.2760	96	1 MHz, 39 kHz
1994 November 10.05–10.30	1.369	0.678	HCN	J(1–0)	88.6318	204	100 kHz, 20kHz
			H_2CO	3_{12}–2_{11}	225.6978	204	100 kHz, 1 MHz, 39 kHz
			CH_3OH	J(3–2)[c]	145.1	204	1 MHz, 39 kHz
JCMT 1994 passage							
1994 November 9.53–9.81	1.368	0.681	HCN	J(4–3)	354.5055	165	378 kHz
			H_2CO	5_{15}–4_{14}	351.7686	165	378 kHz
IRAM 2001 passage							
2001 September 19.26–19.39	1.360	1.487	HCN	J(1–0)	88.6318	160	100 kHz, 20 kHz
2001 September 19.26–19.29			HCN	J(3–2)	265.8864	40	1 MHz, 39 kHz
2001 September 19.26–19.39			H_2CO	3_{12}–2_{11}	225.6978	160	1 MHz, 39 kHz
2001 September 19.26–19.29			CS	J(3–2)	146.9690	40	1 MHz, 39 kHz
2001 September 20.16–20.50	1.360	1.484	HCN	J(1–0)	88.6318	265	100 kHz, 20 kHz
			HCN	J(3–2)	265.8864	265	1 MHz, 39 kHz
			H_2CO	3_{12}–2_{11}	225.6978	265	1 MHz, 39 kHz
			H_2S	1_{10}–1_{01}	168.7628	265	1 MHz, 20 kHz
2001 September 21.18–21.49	1.360	1.480	HCN	J(1–0)	88.6318	285	1 MHz, 100 kHz, 20 kHz
2001 September 21.26–21.49			HCN	J(3–2)	265.8864	165	1 MHz, 39 kHz
2001 September 21.18–21.49			CO	J(2–1)	230.5380	225	1 MHz, 39 kHz
2001 September 21.26–21.49			CS	J(3–2)	146.9690	165	1 MHz, 39 kHz
2001 September 24.16–24.34	1.363	1.468	HCN	J(3–2)	265.8864	145	1 MHz, 39 kHz
			CS	J(3–2)	146.9690	290	1 MHz, 100 kHz, 20 kHz
			CS	J(5–4)	244.9356	145	1 MHz, 39 kHz

[a] Integration time.
[b] 1 MHz: 1 MHz filterbank; 100 kHz: 100 kHz filterbank; 20, 39, 378 kHz: autocorrelator with 20, 39, and 378 kHz resolutions, respectively.
[c] Same CH_3OH lines as on November 8, 1994.

230.5380 GHz) did not yield detections. Results of observations for individual lines, when averaging over all dates, are shown in Table 2. The average line shifts given in Tables 2 and 3 are -0.18 km s^{-1}.

2.2. Observations at JCMT

The observations at JCMT were carried out on November 9.7, 1994 UT. The comet was tracked using the same orbital elements as for IRAM observations, with estimated pointing offsets of $\sim 3.5''$.

The double-sideband B3i receiver operating between 300 and 380 GHz was tuned to cover the HCN J(4–3) (354.5055 GHz) and H_2CO 5_{15}–4_{14} (351.7686 GHz) lines in the signal and image bands, respectively. The observation mode was beam-switching at a rate of 1 Hz and a throw of $150''$. We used a 2048-channel hybrid autocorrelation spectrometer adjusted to a bandwidth of 500 MHz and a spectral resolution of 378 kHz (0.32 km s^{-1} at 354 GHz). At the observed frequencies, the HPBW of the JCMT is $13.5''$. A beam efficiency of ~ 0.6 was estimated from observations of Mars.

The HCN line was easily detected with a signal-to-noise ratio of 13 (Fig. 1; Table 2). No hint of detection is seen for the H_2CO line.

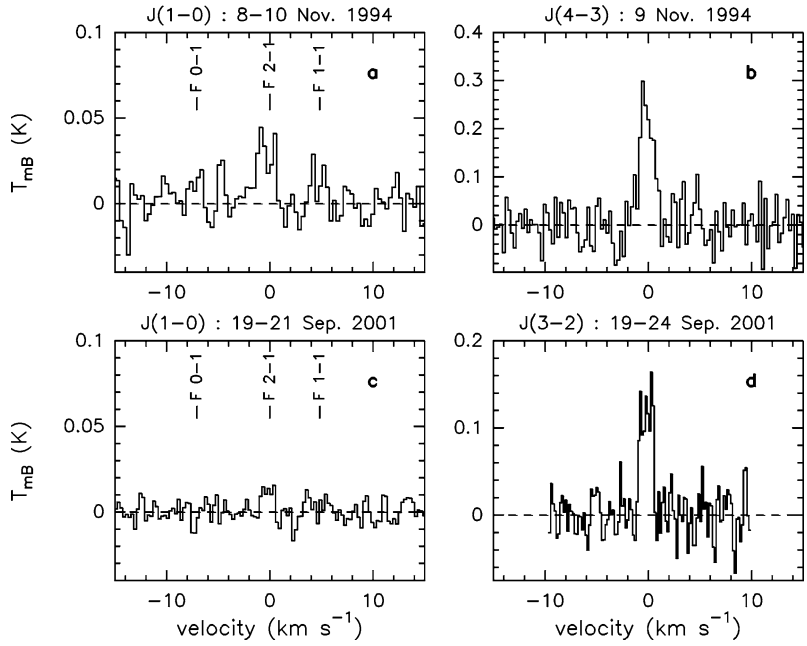

Fig. 1. The HCN lines observed in Comet 19P/Borrelly at IRAM 30-m (a, c, d) and JCMT (b).

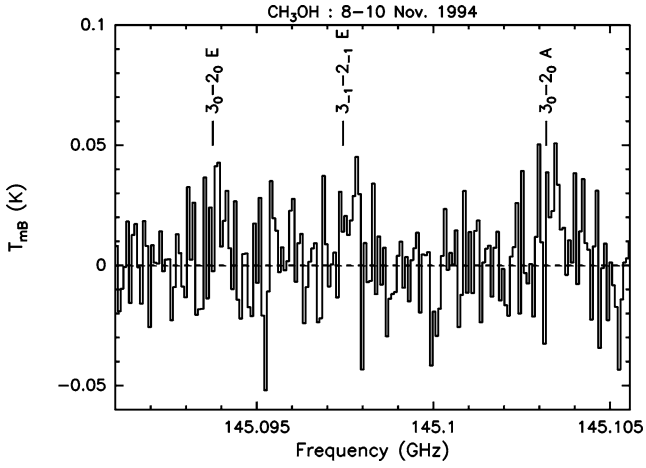

Fig. 2. Three lines of the CH_3OH 145 GHz multiplet observed in Comet 19P/Borrelly in 1994.

2.3. Observations of H_2O with Odin

The 1_{10}–1_{01} fundamental rotational line of ortho water at 556.936 GHz was observed in 19P/Borrelly with Odin. Odin is a small spacecraft launched in February 2001, and includes a 1.1 m antenna equipped with several millimeter and submillimeter receivers (Frisk et al., 2003). Two receivers (549A1 and 555B2) are tunable to the 557 GHz H_2O line. Odin detected water in several comets in 2001 and 2002, as reported by Lecacheux (2001), Lecacheux and Biver (2002), and Lecacheux et al. (2003). With respect to the Submillimeter Wave Astronomy Satellite (SWAS), which first observed the 557 GHz water line in Comet C/1999 H1 (Lee) (Neufeld et al., 2000; Chiu et al., 2001), Odin offers better sensitivity and higher spectral resolution capabilities (up to 80 m s^{-1} at 557 GHz).

The observations of 19P/Borrelly were performed on September 22, 23, and 24, 2001, and on November 5, 2001 (Table 4). The two receivers 549A1 and 555B2 tuned to the 557 GHz water line were used in parallel, each of them connected to an autocorrelation spectrometer set to a total bandwidth of 100 MHz and 140 kHz (80 m s^{-1}) resolution. The signal received at the 555B2 receiver was also analyzed by an acousto-optical spectrometer, which provided a 1.05 GHz bandwidth and 1.0 MHz resolution. The system temperature was $\sim$ 3000 K for both receivers. The HPBW at 557 GHz is 2.2′, and the beam efficiency is $\sim$ 0.9.

The observations consisted of nine-point grids in RA $\times$ Dec coordinates centered on the predicted comet position, with 60″ spacing in September, and 15″ in November. These small maps (4′ $\times$ 4′ and 2.5′ $\times$ 2.5′, respectively) were aimed to overcome pointing offsets due to instrumental effects, known at that time but still out of control. The reconstruction of the attitudes of the pointing system allowed us to provide the exact positions of the telescope pointings, with an accuracy better than 10″. Figure 4 shows the spectra obtained on the nine-point grid in September. The central position of the grid is offset with respect to the nucleus position by $\sim$ 25″ on average in September (Fig. 4), and by 35″ on November 5. Table 4 lists line intensities after averaging radially over a range of offset positions. Figure 5 shows average spectra obtained for the September and November periods.

2.4. Observations at the Nançay radio telescope

The OH 1665 and 1667 MHz lines were observed daily in 19P/Borrelly at the Nançay radio telescope from Septem-

Table 2
Observations at IRAM 30-m and JCMT: results from average spectra

Date	Telescope	Molecule	Line	Area[a] (K km s^{-1})	V_0 (km s^{-1})	Production rate (s^{-1})
1994 passage						
8–10 November 1994	IRAM 30-m	HCN	J(1–0)	0.103 ± 0.014	-0.29 ± 0.09	$(3.4 \pm 0.5) \times 10^{25}$
9.7 November 1994	JCMT	HCN	J(4–3)	0.410 ± 0.032	-0.19 ± 0.07	$(3.8 \pm 0.3) \times 10^{25}$
9.7 November 1994	JCMT	H_2CO	5_{15}–4_{14}	< 0.095	–	$< 2.3 \times 10^{26}$[b]
8–10 November 1994	IRAM 30-m	H_2CO	3_{12}–2_{11}	0.064 ± 0.018	–	$(1.2 \pm 0.3) \times 10^{26}$[c]
8–10 November 1994	IRAM 30-m	CH_3OH	3_0–2_0 E	0.029 ± 0.009	-0.28 ± 0.12	$(4.5 \pm 1.5) \times 10^{26}$
			3_{-1}–2_{-1} E	0.028 ± 0.009		
			3_0–2_0 A	0.038 ± 0.009		
			$3_{\pm2}$–$2_{\pm2}$ E	0.032 ± 0.010		
			3_2–2_2 A^-	< 0.029	–	–
			3_1–2_1 E	< 0.029	–	–
			3_2–2_2 A^+	< 0.029	–	–
9.1 November 1994	IRAM 30-m	CH_3OH	6_0–6_{-1}	< 0.129	–	–
			5_0–5_{-1} E	< 0.123	–	–
			4_0–4_{-1} E	0.131 ± 0.044	–	$(8.5 \pm 2.6) \times 10^{26}$
			1_0–1_{-1} E	< 0.132	–	
			3_0–3_{-1} E	< 0.132	–	
			2_0–2_{-1} E	< 0.132	–	
2001 passage						
19–21 September 2001	IRAM 30-m	HCN	J(1–0)	0.028 ± 0.005	-0.19 ± 0.12	$(1.9 \pm 0.3) \times 10^{25}$
19–24 September 2001	IRAM 30-m	HCN	J(3–2)	0.205 ± 0.013	-0.18 ± 0.04	$(2.3 \pm 0.2) \times 10^{25}$
23–24 September 2001	IRAM 30-m	CS	J(3–2)	0.024 ± 0.007	0.00 ± 0.21	$(1.9 \pm 0.5) \times 10^{25}$
24.3 September 2001	IRAM 30-m	CS	J(5–4)	0.089 ± 0.022	-0.14 ± 0.16	$(3.1 \pm 0.8) \times 10^{25}$
20.3 September 2001	IRAM 30-m	H_2S	1_{10}–1_{01}	0.025 ± 0.012	–	$< 1.5 \times 10^{26}$
21.3 September 2001	IRAM 30-m	CO	J(2–1)	< 0.046	–	$< 4.5 \times 10^{27}$
19-20 September 2001	IRAM 30-m	H_2CO	3_{12}–2_{11}	< 0.037	–	$< 1.2 \times 10^{26}$[d]

[a] In the scale of main beam brightness temperature.
[b] Assuming extended source, $Q[H_2CO] < 5.6 \times 10^{25}$ s^{-1} for nuclear source.
[c] $(3.3 \pm 0.9) \times 10^{25}$ s^{-1} for nuclear source.
[d] $< 5.2 \times 10^{25}$ s^{-1} for nuclear source.

Table 3
HCN observations at IRAM 30-m during DS1 flyby: daily results

Date	Line	Area* (K km s^{-1})	V_0 (km s^{-1})	Production rate (10^{25} s^{-1})
19.3 September 2001	J(1–0)	0.042 ± 0.018	–	2.9 ± 1.2
	J(3–2)	< 0.51	–	< 5.9
20.3 September 2001	J(1–0)	0.035 ± 0.009	-0.35 ± 0.18	2.4 ± 0.6
	J(3–2)	0.197 ± 0.019	-0.17 ± 0.05	2.3 ± 0.2
21.3 September 2001	J(1–0)	0.020 ± 0.009	–	1.4 ± 0.6
	J(3–2)	0.206 ± 0.025	-0.19 ± 0.08	2.4 ± 0.3
24.3 September 2001	J(3–2)	0.184 ± 0.028	-0.07 ± 0.08	2.1 ± 0.3

* In the scale of main beam brightness temperature.

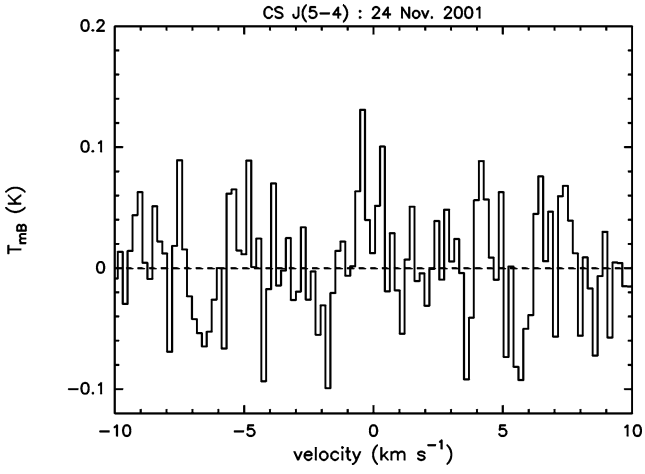

Fig. 3. Spectrum of the J(5–4) line of CS observed on September 24, 2001 in Comet 19P/Borrelly.

ber 5, 1994 to October 11, 1994, and from January 4 to 18, 1995. These observations and their reduction are discussed in Crovisier et al. (2002a).

The comet was observed at its 2001 passage using a new focal system, which improves the sensitivity of the telescope by a factor ~ 2 (Crovisier et al., 2002b). The observations were performed from July 19 to September 3, 2001, and were successful over the entire period. The monitoring was resumed post-perihelion in November, but the comet was no longer detectable, as was the case for the corresponding post-perihelion observations during the 1994 passage. Because of unfavorable OH excitation conditions, observations during the DS1 flyby would not have been useful and were not scheduled. Results and average spectra are presented in Table 5 and Fig. 6, respectively. Note that Table 5 provides the velocity shift V_0 of the OH lines after removing the velocity offset due to the Greenstein effect (Despois et al., 1981).

Table 4
Observations of the H_2O 1_{10}–1_{01} line with Odin

Date (UT)	r_h (AU)	Δ (AU)	t_{int}[a] (min)	Mean offset ($''$)	Area[b] (K km s^{-1})	V_0 (km s^{-1})	Q[H_2O] (10^{28} s^{-1})
2001 September 22.31–22.54	1.361	1.475	72	34 ± 4	0.53 ± 0.10	0.01 ± 0.13	2.5 ± 0.5
2001 September 23.26–23.42	1.362	1.472	68	33 ± 4	1.03 ± 0.11	-0.03 ± 0.08	4.9 ± 0.5
2001 September 24.20–24.43	1.363	1.468	68	32 ± 5	0.59 ± 0.11	-0.01 ± 0.13	2.7 ± 0.5
2001 November 5.48–5.57	1.483	1.340	111	37 ± 13	0.53 ± 0.09	0.08 ± 0.13	2.3 ± 0.4
Average September							
2001 September 22.31–24.43	1.362	1.472	203	32 ± 7	0.69 ± 0.06	0.05 ± 0.06	3.2 ± 0.3
			272	71 ± 11	0.37 ± 0.06	-0.11 ± 0.11	3.0 ± 0.5
			198	103 ± 8	0.29 ± 0.05	-0.27 ± 0.13	4.8 ± 0.8

[a] Integration time.
[b] In the scale of main beam brightness temperature.

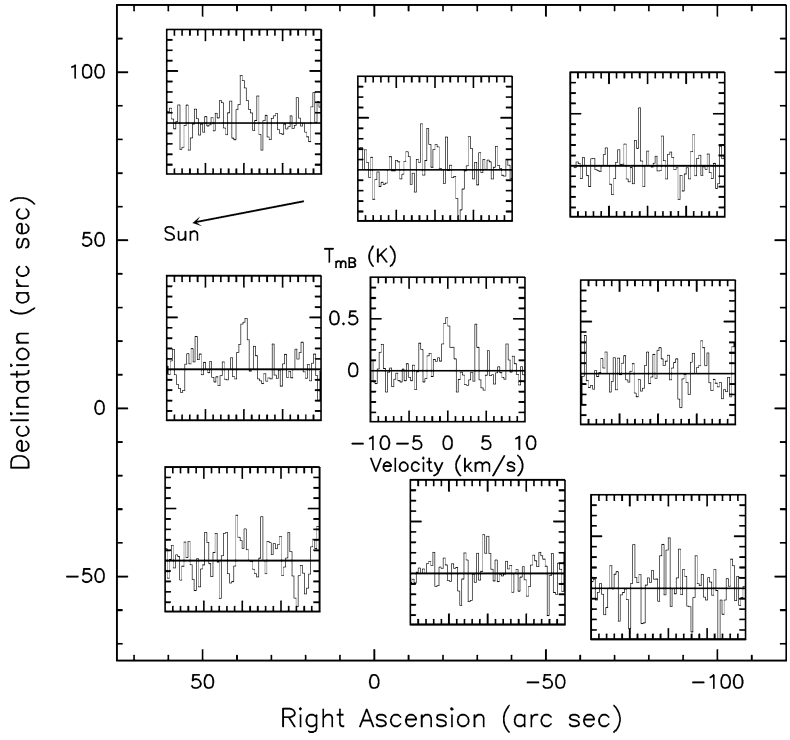

Fig. 4. The 1_{10}–1_{01} H_2O line at 557 GHz observed in Comet 19P/Borrelly with the Odin satellite (mean of 22, 23, and 24 September 2001 observations). The spectra within the boxes correspond to different beam offsets relative to the comet nucleus. For each spectrum, the x-axis is the velocity scale and the y-axis is the brightness temperature scale shown on the central spectrum. The xy boxes are centred on the corresponding RA × Dec beam offsets. The arrow shows the Sun direction.

3. Molecular production rates and abundances

3.1. Production rates of HCN, CH_3OH, H_2CO, CO, H_2S, and CS

Production rates or 3-σ upper limits derived from the millimeter observations are given in Tables 2 and 3. We used excitation models that take into account collisions with water and electrons and IR excitation by the Sun (Biver et al., 1999a, 2000). To model collisional excitation, we adopted a kinetic temperature T_k of 40 K. Such a low kinetic temperature might be expected for a comet with a water production rate $\sim 3 \times 10^{28}$ s^{-1} at $r_h = 1.4$ AU (Section 3.2), based on previous determinations for several comets having various levels of gaseous activity (Biver, 1997; Biver et al., 1999a, 2000). The model for collisional excitation by electron impacts developed by Biver (1997) (see also Biver et al., 1999a) computes electron densities from values measured in 1P/Halley and appropriate scaling laws relative to Q[H_2O] and r_h. Electron densities are multiplied by a parameter x_{ne} to investigate lower or higher values with respect to the nominal case $x_{ne} = 1$. This free parameter, which is directly related to the size of the collisional region at thermal equilibrium, could, in principle, be constrained by the data (e.g., by comparing intensities of different rotational lines of the same molecule (Biver et al., 1999a, 2000)). However,

Table 5
Observations of OH at the Nançay radio telescope

Date (yymmdd)	Δ (AU)	r_h (AU)	$\dot{r}_h$ (km s^{-1})	inv[a]	inv[b]	T_{bg}[c] (K)	Area (mJy km s^{-1})	V_0[d] (km s^{-1})	V_0[d,e] (km s^{-1})	dV_0[d] (km s^{-1})	Q[OH][f] (10^{28} s^{-1})
1994 passage											
940905–940919	1.13	1.48	−7.5	−0.31	−0.37	3.4	-32 ± 6	0.07 ± 0.17	0.08 ± 0.17	1.98 ± 0.43	1.5 ± 0.3
940920–940929	1.01	1.43	−6.0	−0.28	−0.33	3.4	-69 ± 8	-0.09 ± 0.13	-0.03 ± 0.12	2.22 ± 0.31	2.8 ± 0.3
940930–941011	0.92	1.40	−4.4	−0.22	−0.26	3.5	-48 ± 7	-0.21 ± 0.11	-0.14 ± 0.11	1.79 ± 0.27	2.3 ± 0.4
950104–950118	0.75	1.58	9.5	−0.15	−0.14	3.2	-9 ± 7				< 1.4
2001 passage											
010719–010801	1.81	1.48	−7.6	−0.31	−0.37	3.3	-15 ± 3	0.10 ± 0.17	0.11 ± 0.17	1.89 ± 0.42	1.1 ± 0.2
010802–010815	1.71	1.42	−5.7	−0.27	−0.32	3.5	-17 ± 4	-0.17 ± 0.14	-0.12 ± 0.15	1.46 ± 0.34	1.4 ± 0.3
010816–010822	1.65	1.39	−4.3	−0.22	−0.25	3.5	-28 ± 5	-0.25 ± 0.20	-0.12 ± 0.20	2.00 ± 0.49	2.4 ± 0.5
010822–010903	1.59	1.37	−2.7	−0.13	−0.14	3.5	-17 ± 3	-0.52 ± 0.17	-0.27 ± 0.12	1.75 ± 0.42	2.3 ± 0.4
011111–011129	1.31	1.56	9.3	−0.14	−0.13	3.4	< 9				< 0.9

[a] Maser inversion from Despois et al. (1981).
[b] Maser inversion from Schleicher and A'Hearn (1988).
[c] Background temperature.
[d] Width (dV_0), and centre (V_0) from gaussian fit.
[e] Centre after removing the velocity offset due to Greenstein effect.
[f] OH production rate using the maser inversion from Despois et al. (1981), collisional quenching and an Haser-equivalent model for OH distribution (Crovisier et al., 2002a). The Haser-equivalent scalelengths correspond an expansion velocity of 0.8 km s^{-1} for H_2O, an ejection velocity of 0.95 km s^{-1} for OH, a photodissociative lifetime of 1.1×10^5 s at $r_h = 1$ AU for OH, and a H_2O lifetime which varies with solar activity from Crovisier (1989).

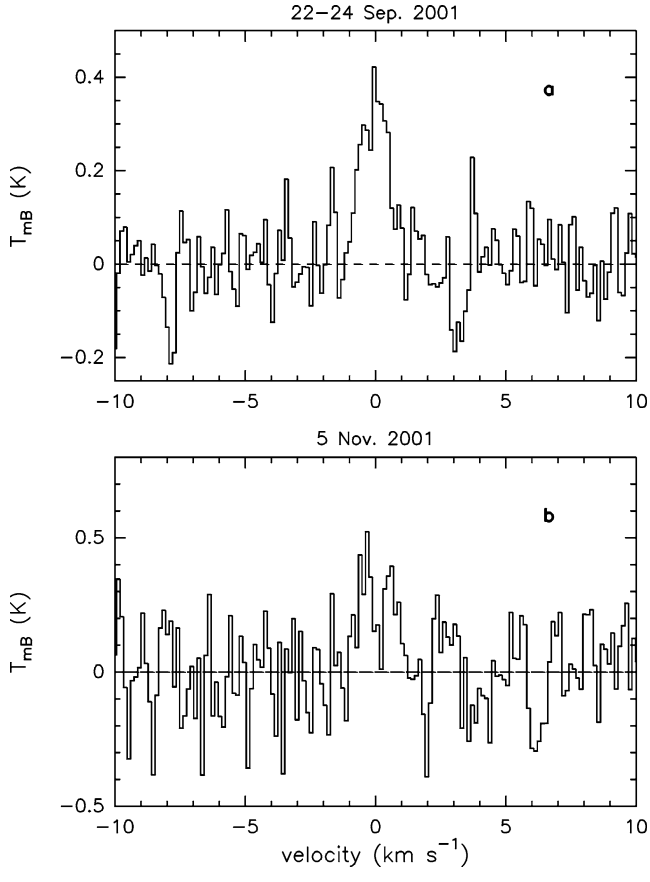

Fig. 5. The 1_{10}–1_{01} H_2O line at 557 GHz observed in Comet 19P/Borrelly with the Odin satellite: (a) average of 22, 23, 24 September 2001 observations with position offsets between 30″ and 90″; (b) observations on November 5, 2001 with mean position offset of 39″. Spectra have been smoothed to a spectral resolution of 0.13 km s^{-1}.

the signal-to-noise ratios obtained on the HCN and CH_3OH lines observed in 19P/Borrelly are too low to provide strong constraints. Production rates given in Tables 2 and 3 assume $x_{ne} = 0.2$, a value dictated by the recent observations of the H_2O 557 GHz line (see Section 3.2). Values differing by at most 20% are obtained when varying the kinetic temperature and the x_{ne} parameter over the ranges $T_k = 30$ to 60 K and $x_{ne} = 0$ to 1, which provide reasonable agrement among the different HCN and CH_3OH lines.

Our calculations assume an isotropic coma and an expansion velocity of 0.75 km s^{-1}. This outflow velocity is consistent with the half-power width of the HCN lines. However, their asymmetrical shape suggests anisotropies of the gas expansion velocity and/or outgassing in the coma. This will be further discussed in Section 4. For all molecules, except CS and H_2CO, we used parent molecule distributions. The assumed photodissociation rates take into account the solar activity in 1994 and 2001. The adopted photodissociation rates are $1.34 \times 10^{-5} r_h^{-2}$ s^{-1} for the 1994 observation period and $2.1 \times 10^{-5} r_h^{-2}$ s^{-1} for 2001, following Bockelée-Morvan and Crovisier (1985) and Crovisier (1989). For CS in September 2001, we assumed an extended source distribution with a parent scalelength L_p of 500 km, corresponding to production by CS_2. For H_2CO, we assumed $L_p = 11000$ km, following Biver et al. (1999a). H_2CO production rates computed under the assumption of direct release from the nucleus are also given in Table 2.

The Q[HCN] values measured from the J(3–2) observations in 2001 (Table 3) suggest that the average daily gaseous activity of 19P/Borrelly was fairly constant from day to day at the time of the DS1 flyby. The average value deduced for this period from both J(1–0) and J(3–2) lines is $Q(\mathrm{HCN}) = (2.1 \pm 0.2) \times 10^{25}$ s^{-1}.

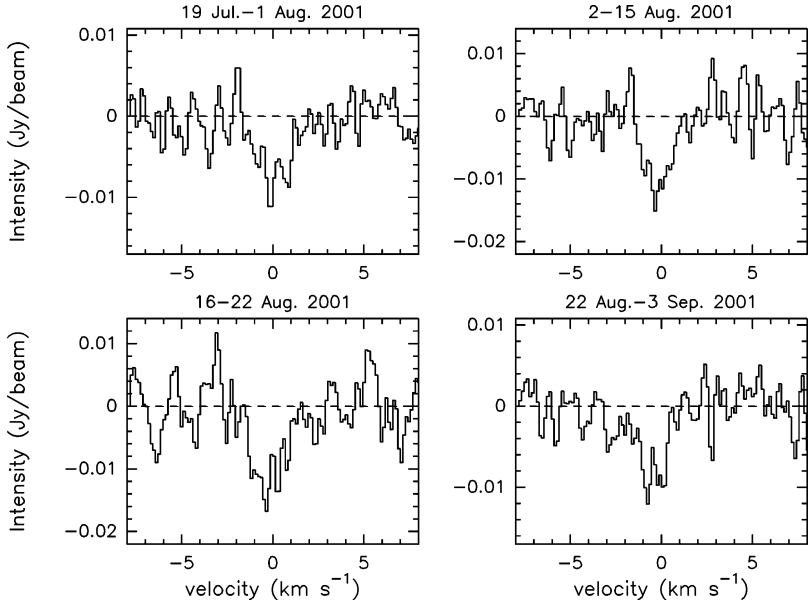

Fig. 6. 18-cm spectra of the OH radical observed in 19P/Borrelly at the Nançay radio telescope in 2001.

3.2. OH and H_2O production rates

OH production rates Q[OH] derived from the Nançay observations are given in Table 5. Resulting H_2O production rates ($Q[H_2O] = 1.1 \times Q$[OH]) are plotted in Fig. 7. They correspond to calculations made with a Haser-equivalent model for the OH-distribution, the Despois et al. (1981) model for the maser inversion *inv*, and collisional quenching. Details on the calculation procedure and model parameters are given in Crovisier et al. (2002a). However, in contrast to this last paper, we varied the H_2O lifetime according to solar activity following Crovisier (1989). Therefore, Q[OH] values for 1994 slightly differ (by 10% at most) from those given in Crovisier et al. (2002a).

The model used to derive the H_2O production rate from the Odin observations shares many similarities with those developed for HCN, CH_3OH, H_2CO, etc. (Section 3.1). The excitation part is an improved version of the model developed by Bockelée-Morvan (1987), which now includes excitation by electron collisions and radiative excitation via the (100), (101), and (011) vibrational states (Chiu et al., 2001). This model treats radiation trapping effects in the excitation using an escape probability method (Bockelée-Morvan, 1987). The H_2O model was run with a x_{ne} parameter equal to 0.2. This value was found to describe correctly the evolution of the H_2O line intensity with beam offset in comets for which extensive mapping has been performed with Odin (e.g., 153P/2002 C1 (Ikeya–Zhang), Lecacheux et al., 2003; Biver et al., in preparation). As for the species considered in Section 3.1, once the populations of the rotational levels are calculated throughout the coma, the intensity of the 557 GHz H_2O line is computed by numerical integration assuming a Haser density distribution. This radiative transfer code takes into account opacity effects, which are important for the water 1_{10}–1_{01} line (optical depth of ~ 0.6 for September 22–24, 2001 at 32″ offset). We used a H_2O photodissociation rate of $2.0 \times 10^{-5} r_h^{-2}$ s^{-1}, which was derived from Crovisier (1989) using the 10.7 cm solar flux at the time of the observations. The resulting water production rates are given in Table 4 and are plotted in Fig. 7. The average production rate derived for this period from the intensity at 103″ offset is somewhat higher than the values deduced for the 32″ and 71″ positions. As the line is only marginally detected at 103″ offset, it is possible that the baseline subtraction procedure overestimates the intensity. Using all offset positions, we derive a weighted mean water production rate of $(3.3 \pm 0.6) \times 10^{28}$ s^{-1} for September 22–24, 2001.

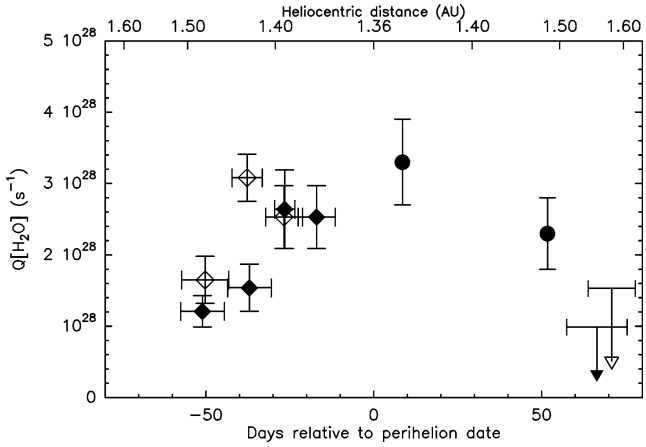

Fig. 7. H_2O production rates in Comet 19P/Borrelly from Nançay (open diamonds: 1994; filled diamonds: 2001) and Odin data (filled circles). Arrows correspond to 3-σ upper limits derived from Nançay observations (open and filled symbols for 1994 and 2001, respectively).

As already noted by Schleicher et al. (2003), the Nançay-Q[OH] values for the 1994 passage are in good agreement with those obtained from narrowband photometry. They vary

between 1.5 and 2.8×10^{28} s^{-1} in the range $r_h = 1.40$–1.48 AU, pre-perihelion. OH production rates measured pre-perihelion in 2001 range from 1.1×10^{28} ($r_h = 1.48$ AU) to 2.4×10^{28} s^{-1} ($r_h = 1.37$ AU). An upper limit of 9×10^{27} s^{-1} is derived for the November 11–29, 2001 period. These values are again consistent with contemporaneous values deduced from narrowband photometry, taking into account the uncertainties (Schleicher et al., 2003). We note that the OH production rates are similar for the 1994 and 2001 apparitions (Fig. 7).

The $Q[H_2O]$ derived from the Odin observations on September 22–24, 2001 are in good agreement with the value of $(3.0 \pm 0.6) \times 10^{28}$ s^{-1} deduced from OH observations with the Hubble Space telescope on September 21 and 23 (Weaver et al., 2003). They are also consistent with the value of 2.5×10^{28} s^{-1} deduced by Schleicher et al. (2003) for September 18–19. Unfortunately, such direct comparison cannot be made for the November 5 measurement. However, the $Q[H_2O]$ values derived by Schleicher et al. (2003) are ~ 1.3 and 0.6×10^{28} s^{-1}, for October 18 ($r_h = 1.41$ AU) and November 14–15, 2001 ($r_h = 1.53$ AU), respectively. These values, together with the steep post-perihelion r_h-dependence they inferred from their whole set of data, suggest a factor of 2 discrepancy with our measurement of $(2.3 \pm 0.4) \times 10^{28}$ s^{-1}. The agreement is not much improved when varying the parameters T_k and x_{ne} of our model within reasonable ranges (note that r_h did not vary much between September and November 2001, so that we do not expect significant variations in the excitation conditions between these two dates). Possibly, both UV and radio determinations are significantly affected by the assumption of an isotropic distribution. As discussed in Section 4, the coma of 19P/Borrelly is strongly anisotropic and the viewing geometry from Earth changed from September to November 2001.

3.3. Comparison between 1994 and 2001 returns

The comparison between the 1994 and 2001 HCN data sets is instructive because both sets were obtained about one week after perihelion at $r_h \approx 1.36$ AU. We find that the HCN production rate was smaller in 2001 than in 1994, by a factor of 1.7. This is not consistent with the results obtained by Schleicher et al. (2003) for OH and CN: when adjusting the Haser-equivalent scalelengths to take into account the difference in solar activity between 1994 and 2001, they find no significant differences in Q[OH] and Q[CN] values for 2001 and 1994 near the dates of the HCN observations. Farnham and Cochran (2002) observed CN and C_2 on September 23, 2001 at the McDonald Observatory, and they also remarked on the similarity with the data obtained on November 8–10, 1994 (Cochran and Barker, 1999) at nearly the same heliocentric distance. This similarity in gas production between the 1994 and 2001 apparitions is observed over several weeks away from perihelion (Schleicher et al., 2003). The Q[OH] values measured at Nançay, though only pre-perihelion, also suggest that 19P/Borrelly displayed similar water outgassing activity in 1994 and 2001 (Fig. 7). We do not have any obvious explanation for this discrepancy with the HCN results. In Section 4 we will show that similar HCN production rates can be obtained for 1994 and 2001, if we adopt a strongly anisotropic distribution for HCN. Since this distribution is not our preferred solution for HCN outgassing (see the next section), we will conservatively adopt the HCN production rates inferred with the isotropic model.

3.4. Molecular abundances

Production rates relative to water are given in Table 6. For the 2001 September data, we used the $Q[H_2O]$ value determined with Odin ($(3.3 \pm 0.6) \times 10^{28}$ s^{-1}). As discussed in the previous section, the water production rate near November 9, 1994 was similar to that near September 22, 2001. For consistency, we also assumed $Q[H_2O] = (3.3 \pm 0.6) \times 10^{28}$ s^{-1} for the 1994 abundance determinations. Using the $Q[H_2O]$ values inferred by Schleicher et al. (2003) from OH observations (2.5×10^{28} s^{-1}) would result in abundances relative to water 30% higher.

The difference in the Q[HCN] and $Q[H_2O]$ behaviors between 1994 and 2001 produces a significant discrepancy in the relative Q[HCN]/$Q[H_2O]$ abundance ratios at the two passages (0.11 and 0.06%, respectively, Table 6). This variation, which is not observed for the CN, C_2, and C_3 radicals (Schleicher et al., 2003), is likely not real.

Our derived Q[HCN]/$Q[H_2O]$ values may be interesting to compare to measured Q[CN]/Q[OH] ratios. Indeed, the presence of sources of CN radicals other than HCN in cometary atmospheres is often invoked, in particular to explain the CN radial distribution which does not agree with that expected from HCN photodissociation. The Q[CN]/Q[OH] values measured in 19P/Borrelly range from $\sim 10^{-3}$ (Hamane et al., 2002) to 2.4×10^{-3} (Schleicher et al., 2003), so it is difficult to conclude anything definite regarding the origin of CN in this comet from the comparison of the HCN and CN abundance ratios. The direct comparison of contemporaneous HCN and CN production rates is also not obvious, and is complicated by the usage of different model parameters, even among the several authors publish-

Table 6
Molecular abundances in 19P/Borrelly

Molecule	$Q/Q[H_2O]$[a] (%)		Q/Q[HCN] (%)	
	1994	2001	1994	2001
HCN	0.11 ± 0.02	0.06 ± 0.01	1	1
CS	–	0.07 ± 0.02	–	1.1 ± 0.2
H_2S	–	< 0.45	–	< 7
CH_3OH	1.7 ± 0.5	–	15 ± 2	–
H_2CO ext.	0.36 ± 0.11	< 0.36	3.3 ± 0.8	< 6
H_2CO nuc.	0.10 ± 0.03	< 0.17	0.9 ± 0.3	< 2.5
CO	–	< 15	–	< 214

[a] Assuming $Q[H_2O] = (3.3 \pm 0.6) \times 10^{28}$ s^{-1} determined from the Odin observations in 2001. The uncertainties include the uncertainty on $Q[H_2O]$.

ing CN production rates. Taken at their face values, the CN production rates inferred by Farnham and Cochran (2002) and Schleicher et al. (2003) near the time of the DS1 flyby are 1.5 to 2.3 times higher than the HCN production rate we derive for the same period.

From the CN radial distribution recorded in September 2001, Farnham and Cochran (2002) derived a Haser-equivalent scalelength for the CN parent of 1.3×10^4 km, when scaled to $r_h = 1$ AU. This value can be compared to the value expected from HCN photodissociation. As discussed by Combi and Delsemme (1980), the excess velocity received by CN during HCN photodissociation must be taken into account. Assuming a CN ejection velocity of 0.9 km s^{-1} (Bockelée-Morvan and Crovisier, 1985), and using the method developed by Combi and Delsemme (1980), we derive a Haser-equivalent scalelength for HCN of 2.7×10^4 km at $r_h = 1$ AU. This is two times larger than the value derived for the CN parent by Farnham and Cochran (Farnham and Cochran, 2002). Therefore, both the Q[CN]/Q[HCN] ratio and the radial distribution of CN suggest that HCN is not the sole parent of CN in this comet. Similar results were obtained for a number of comets (e.g., Bockelée-Morvan and Crovisier, 1985; Festou et al., 1998).

From a comparative study of 24 comets observed at millimeter and submillimeter wavelengths, Q[HCN]/Q[H_2O] was found to vary from 0.08 to 0.25%, with a mean value around 0.13% (Biver et al., 2002). Interestingly, among the sample, only the Jupiter-family Comet 21P/Giacobini–Zinner has a Q[HCN]/Q[H_2O] as low as 0.08% (Biver et al., 1999c), although another Jupiter-family comet, 22P/Kopff, has a slightly higher Q[HCN]/Q[H_2O] value (0.13%). It will be interesting to try to confirm the low Q[HCN]/Q[H_2O] value measured in 19P/Borrelly in 2001 at future apparitions, in order to investigate whether Jupiter-family comets are indeed HCN-depleted. Although only a fraction of the CN radicals may come from HCN, it is worth noting that carbon-depleted comets (about half of the Jupiter-family comets, including 19P/Borrelly) have a lower average Q[CN]/Q[OH] value (0.20%, to be compared to 0.32% for "typical comets"; A'Hearn et al., 1995).

The CH_3OH abundance relative to water, only measured in 1994 (1.7 ± 0.5%, Table 6), agrees with the mean abundance of 2.2% measured among comets (Biver et al., 2002; Mumma et al., 2002). The Q[CH_3OH]/Q[HCN] ratio ($= 15 \pm 4$), which may be more reliable than the Q[CH_3OH]/Q[H_2O] ratio, is somewhat lower that the mean value measured in comets (~ 22) (Biver et al., 2002).

Spectroscopic observations of CO and H_2S in Jupiter-family comets are interesting as such comets may have severe depletions in volatile species due to their numerous passages near the Sun. The derived upper limit on the CO abundance (15%) is not very constraining, although CO appears to be less abundant in 19P/Borrelly than in Comets C/1995 O1 (Hale–Bopp) and C/1996 B2 (Hyakutake). The CO/H_2O abundance ratio varies among comets from less than 1 to ~ 25% (e.g., Biver et al., 2002; Mumma et al., 2002). In Comet 21P/Giacobini–Zinner, the only Jupiter-family comet in which CO has been detected, CO/H_2O is ~ 15% (Mumma et al., 2000). However, Weaver et al. (1999), from similar IR observations, inferred an upper limit of 2–3% consistent with the limit obtained from radio measurements (< 2.5%, Biver et al., 1999c). From millimeter observations, CO/H_2O is less than 6% in the Jupiter-family Comet 22P/Kopff (Biver, 1997). From ultraviolet observations, CO/H_2O is less than 1% in the Jupiter-family Comet 103P/Hartley 2 (Weaver et al., 1994).

With an abundance < 0.45%, H_2S is also less abundant in Comet 19P/Borrelly than in Comets Hale–Bopp and Hyakutake, for which values of 1.5 and 0.8% were measured, respectively (Bockelée-Morvan et al., 2000; Biver et al., 1999a). Among a sample of eleven comets in which H_2S was detected, H_2S/H_2O varies from 0.4 to 1.5% in ten comets, and is only 0.12% in the long-period Comet C/2000 WM_1 (LINEAR) which presents also a strong CO-depletion (Biver et al., 2002). Therefore, the H_2S abundance in 19P/Borrelly is in the low range of measured values. It is interesting to note that 21P/Giacobini–Zinner is also H_2S-poor (< 0.4%, Biver et al., 2002). However, this is not the case for 22P/Kopff, which has a H_2S/H_2O ratio of 0.6% (Biver, 1997; Biver et al., 2002).

Many more Jupiter-family comets must be sampled to establish whether they present distinct chemical properties with respect to Oort cloud comets.

4. Line shapes and gas distribution

The high-resolution images obtained by DS1 of 19P/Borrelly revealed a highly elongated, 8-km long nucleus in agreement with the earlier measurement from the *Hubble Space Telescope* of 3.6×8.8 km (Soderblom et al., 2002; Lamy et al., 1998). The images also showed that the dust emission in the inner coma was dominated by a narrow bright jet, called the α-jet, directed along the nucleus short-axis and only a few hundred meters in width at its base. Soderblom et al. (2002) concluded that this jet was nearly aligned with the rotation axis, as its direction remained stationary during the DS1 approach. The α-jet's equatorial coordinates ($RA = 218.5 \pm 3°$, $Dec = -12.5 \pm 3°$) place the sub-solar latitude at 55° North and the sub-Earth latitude at 13° North, assuming that this jet emanates from the North pole.

Independently, images of the dust coma obtained from ground-based telescopes showed a strong straight primary jet, which persisted over a few months (Farnham and Cochran, 2002; Schleicher et al., 2003). The same jet was observed at the 1994 and previous apparitions. The lack of curvature in the jet led these authors to suggest that the jet was emanating near the pole. By modelling the measured position angle of this jet as a function of time during the 1994 and/or 2001 passages, Farnham and Cochran (2002) and Schleicher et al. (2003) concluded that it can be associ-

ated with the α-jet. They determined the orientation of the spin axis to be RA = 214°, Dec $\sim -(5$–$6)°$. Samarasinha and Muller (2002) obtained a set of solutions centered on RA = 221°, Dec $\sim -7°$, which encompasses the other determinations. Schleicher et al. (2003) showed that this spin orientation implies strong seasonal effects in the illumination of the jet's polar source, which explains both the jet's appearance and the water production curve they observed in the few weeks preceding and following perihelion. They concluded that the polar source contributed $\geqslant 90\%$ of the total water production near perihelion.

The velocity offset and shape of the radio line profiles provide information on the gas distribution along the line of sight. It is thus interesting to investigate how this gas distribution compares with the dust distribution and if the results on the gas distribution are consistent with the results quoted above.

Our most reliable information is derived from the HCN lines. The signal-to-noise ratios on the OH lines are poorer (see later discussion), and the H_2O profiles are affected by self-absorption effects caused by the opacity of the H_2O 557 GHz line. Self-absorption is more important in the blue wing of the H_2O line than in the red one, and this results in a net displacement of the line towards red velocities. This effect was evident in high quality H_2O 557 GHz spectra of Comets C/2001 A2 (LINEAR) and C/2002 C1 (Ikeya–Zhang) (Lecacheux et al., 2003) and could be explained quantitatively by modelling. In the case of 19P/Borrelly on September 22–24 at 32″ offset from the nucleus, we expect a net line displacement $\Delta V_0 = +0.09$ km s^{-1} from our radiative transfer model, assuming an isotropic H_2O coma. This partly explains the difference in velocity shifts between the HCN and H_2O line profiles, $V_0 = -0.18 \pm 0.04$ km s^{-1} and $V_0 = 0.05 \pm 0.06$ km s^{-1}, respectively, in September 2001. It is difficult to know whether the remaining slight discrepancy between the HCN and H_2O line offsets reflects differences in HCN and H_2O spatial distributions or a failure of our radiative transfer treatment. Qualitatively, better agreement should be obtained with an anisotropic model, which provides blueshifted lines under optically thin conditions.

Interestingly, the HCN observations in 1994 and 2001 were made under almost identical geometrical conditions. The Earth–comet–Sun angles were similar ($\sim 44°$ and $\sim 41°$ for 1994 and 2001, respectively), as was the orientation of the spin axis with respect to the comet–Earth vector as determined by Schleicher et al. (2003). The remarkable similarity in the Doppler shifts of the HCN lines in 1994 and 2001 suggests a similar outgassing pattern of the nucleus at the two apparitions, as observed for the dust coma morphology.

Next, we can examine the kind of outgassing pattern that could explain the HCN line profiles. In a first approximation, the line velocity shift is simply the projection along the line of sight of the net velocity vector $(\mathbf{v}_p)_z$ of all HCN molecules outflowing from the nucleus (in fact, as the HCN coma is resolved by the beam, more HCN molecules moving towards or away from the Earth are confined within the beam, so that $|V_0| \gtrsim |(\mathbf{v}_p)_z|$). Then, if we consider the extreme and simplistic case where the HCN distribution is confined within a cone, the line velocity shift is approximately equal to $v_{\rm exp} \cos\theta \cos\phi$, where θ is the half-opening angle of the cone, ϕ is the angle between the cone axis and Earth direction, and $v_{\rm exp}$ is the HCN radial expansion velocity. Assuming $v_{\rm exp} = 0.75$ to 0.9 km s^{-1} and θ in the range 0°–45°, $V_0 = -0.18 \pm 0.04$ km s^{-1} can be matched with ϕ from 65° to 81°. As any broader HCN angular distribution will tend to symmetrize the spectrum, these simple calculations show that preferential HCN outgassing along the α-jet direction (which is at $\phi = 77°$) is consistent with our data, providing most HCN molecules sampled by the beam (typically those at a few thousand kilometers) are confined within a limited angular extent. On the other hand, broader angular distributions with net velocity vector $\mathbf{v}_p$ closer to the comet–Earth direction (e.g., towards the Sun) are also allowed.

To go further in the analysis, we have computed synthetic spectra where the HCN density distribution in the coma is described as the superimposition of an emission cone characterized by (θ, ϕ), and an isotropic emission. The radial dependence in these two components follows the Haser variation. The same distribution is used for H_2O, which results in increased collision rates along the cone. The production rate in the jet relative to the isotropic component $Q_{\rm jet}/Q_{\rm iso}$ is a free parameter which can be adjusted to fit the observed velocity shift of the HCN line. The total production rate $Q[\mathrm{HCN}] = Q_{\rm jet} + Q_{\rm iso}$ is constrained by the intensity of the line. The model takes into account thermal broadening of the line at T_k.

Figure 8 shows examples of synthetic line profiles superimposed on the best observed HCN lines (J(4–3) for 1994 and J(3–2) for 2001). We fixed the gas expansion velocity in the isotropic component to 0.65 km s^{-1} and in the conical jet to 0.9 km s^{-1}. These values are the minimum ones needed to fit the widths at half maximum of the red and blue wings of the HCN lines, respectively. The half-opening angle of the jet was taken equal to $\theta = 30°$. Values in the range $\theta = 15°$–$45°$ do not change the results very much. Three values of the angle ϕ between the line of sight and this gas jet were investigated:

(1) $\phi = 15°$, which is close to the Earth direction. In this case, $Q_{\rm jet}/Q[\mathrm{HCN}] = 19\%$, which corresponds to a factor 3.6 enhancement of the local density in the jet;
(2) $\phi = 45°$, which is close to the Earth–comet–Sun angle and simulates outgassing in the solar direction. The required fraction of outgassing in the jet is $Q_{\rm jet}/Q[\mathrm{HCN}] \approx 30\%$. The total production rates Q[HCN] are not very different from the values deduced with the isotropic model: 3.1×10^{25} s^{-1} is inferred from the 1994 J(4–3) line, and 2.0×10^{25} s^{-1} from the 2001 J(3–2) data;
(3) $\phi = 75°$, which is roughly the direction of the α-jet in 1994 and 2001. The required $Q_{\rm jet}/Q[\mathrm{HCN}]$ ratio is 90% for the two dates, with $Q[\mathrm{HCN}] = 3.2 \times 10^{25}$ s^{-1} in

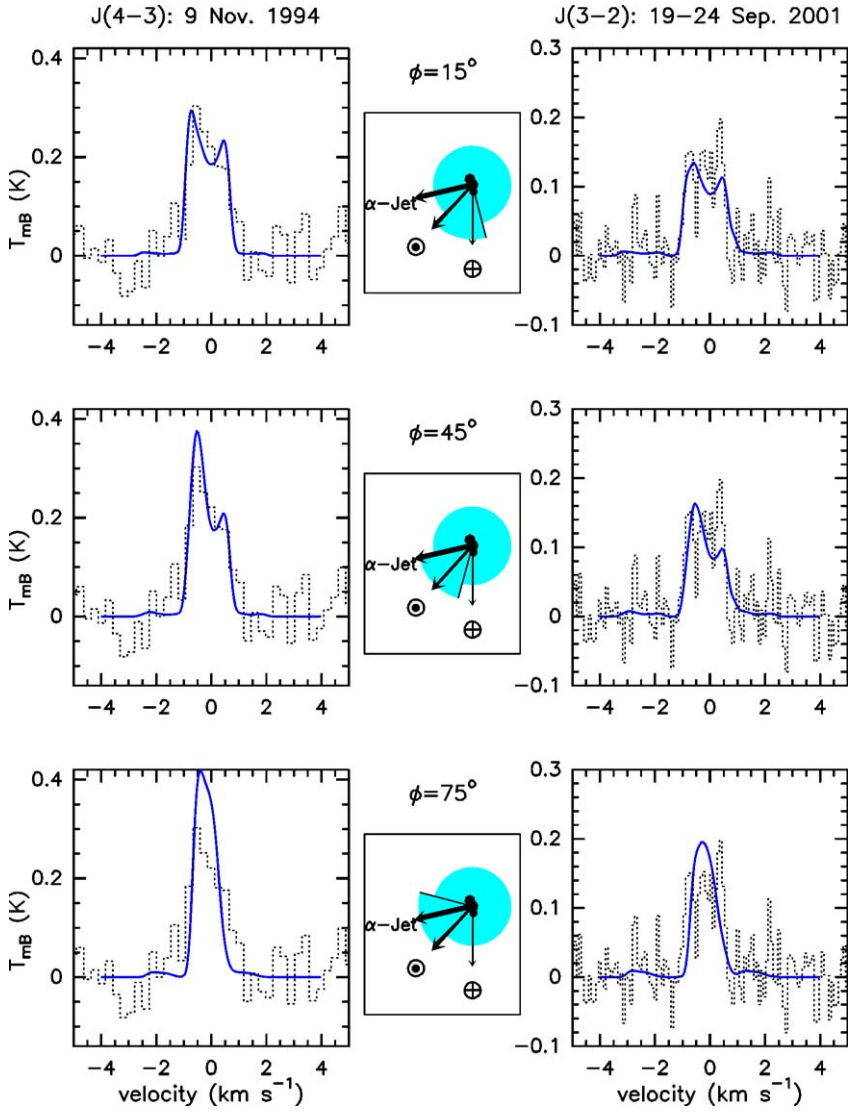

Fig. 8. Synthetic spectra (plain lines) superimposed on the HCN lines of Comet 19P/Borrelly observed at JCMT in November 1994 and IRAM in September 2001 (dashed lines). The central figures depict the geometry of the outgassing adopted with respect to the α-jet direction observed by DS1, the comet–Sun and comet–Earth vectors. All three vectors are nearly in the ecliptic plane. The shaded sectors represent the isotropic and jet components where expansion velocities are 0.65 and 0.9 km s^{-1}, respectively. The half-opening angle of the jet component is $\theta = 30°$. The three sets of figures correspond to $\phi = 15°$, 45°, and 75°, from top to bottom, where ϕ is the angle between the jet axis and Earth direction. The relative production rate in the jet with respect to the total production rate $Q_{\rm jet}/Q$[HCN] is 19, 30, and 90%, from top to bottom.

1994 and Q[HCN] $= 3.0 \times 10^{25}$ s^{-1} in 2001. Therefore, this model provides similar Q[HCN] values for 1994 and 2001, in contrast to the isotropic model used for the calculations given in Tables 2 and 3. Indeed, with this strong anisotropic distribution, the peak brightness of HCN emission is strongly shifted towards the position angle of the jet at PA = 94°. The pointing offset of the 1994 HCN observations, which is taken into account in the calculation of production rates, was fortuitously towards about the same PA (Section 2.2). In contrast, we expect that the beam was aimed at the nucleus position in 2001: hence the higher HCN production rate inferred in the anisotropic model since, in this case, the beam was offset with respect to the peak HCN brightness. Figure 8 shows that this outgassing geometry does not provide the best fit to the line shapes. However, it is possible to better reproduce the blue wing of the line by assuming an expansion velocity in the jet higher than 0.9 km s^{-1}. Taking $v_{\rm exp} = 1.1$ km s^{-1} in the jet indeed improves the fit, and results in $Q_{\rm jet}/Q$[HCN] $\approx 75\%$ and Q[HCN] $\approx 3.7 \times 10^{25}$ s^{-1} for both periods (Fig. 9).

This last case, which would indicate similarities between the mean orientation of the HCN distribution and that of the α-jet, may not be realistic given the high HCN velocity required to fit the data. With $\theta = 30°$, the local H_2O density in the jet is equivalent to that obtained with a H_2O production rate $\sim 4 \times 10^{29}$ s^{-1} in 4π steradians. For com-

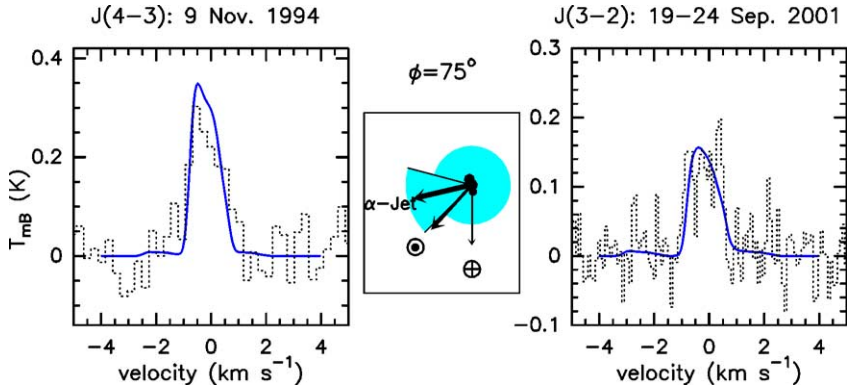

Fig. 9. Synthetic spectra (plain lines) superimposed on the HCN lines of Comet 19P/Borrelly observed at JCMT in November 1994 and IRAM in September 2001 (dashed lines) (see Fig. 8). The expansion velocities in the isotropic and jet components are 0.65 and 1.1 km s^{-1}, respectively. The half-opening angle of the jet component is $\theta = 30°$. The angle between the jet axis and Earth direction is $\phi = 75°$. The value of $Q_{\rm jet}/Q$[HCN] is $\sim 75\%$.

parison, the largest $v_{\rm exp}$ ever measured from millimetric line shapes at $r_h \sim 1.4$ AU was in Comet Hale–Bopp, with $v_{\rm exp} = 0.9$ km s^{-1} for $Q[{\rm H_2O}] \approx 2 \times 10^{30}$ s^{-1} (Biver et al., 1999b). Another interesting comparison is with Comet 109P/Swift–Tuttle, as this comet displayed strong jet-like structures both in optical images (Jorda et al., 1994) and radio spectra (Bockelée-Morvan et al., 1994a, 1994b; Despois et al., 1996) at its 1992 perihelion. From a study of the HCN line shape similar to that performed here, Biver (1997) determined an outflow velocity in the HCN jet-component of 109P/Swift–Tuttle of 1.1 km s^{-1} on November 21, 1992. However, the comet was at $r_h = 1.02$ AU and the HCN production rate $Q_{\rm jet}$ inferred within the jet is more than ten times stronger than that of 19P/Borrelly (Biver, 1997).

Strong outgassing along the α-jet direction also seems to be in conflict with the velocity shifts of the OH lines. From mid-July to the end of August 2001 (i.e., the period of the Nançay observations), the angle between the Sun and α-jet directions remained between 15 and 19°, while it was 35° on September 22 at the time of the HCN observations. Therefore, the base of the α-jet at the nucleus surface was more insolated during the OH observations. More importantly, the Earth–comet-jet angle, ϕ, was smaller during the Nançay period than during the HCN observations: ϕ increased from 33° to 57° over August 2001, compared to the value of 77° on September 22. If outgassing occurred towards the α-jet direction, we then would have expected the OH lines to be significantly more blueshifted than the HCN lines observed in September. (Scaling V_0 according to $\cos\phi$, we expect up to a factor of 3 difference in the absolute values of the velocity shifts between mid-August and September data.) The same study for September–November 1994 shows that these arguments also apply to the 1994 passage. Such a trend is not seen in the data (column 10 in Table 5). Rather, the opposite is observed, although the signal-to-noise ratios of the Nançay lines are not large enough to be confident of this trend. In contrast to the Earth–comet-jet angle, the phase angle did not vary much from mid-July to September 2001 (34 to 41°). Therefore, preferential outgassing towards the Sun is consistent with the OH data.

Coming back to the alternative in which H_2O outgassing occurs preferentially along the α-jet direction, it may be argued that the small OH velocity shifts might result from a significant contribution to the H_2O coma of icy sublimating grains moving at small velocities (in contrast, the HCN molecules would sublimate mainly from the nucleus owing to their higher volatility). This was observed in Comet Hale–Bopp, when at large heliocentric distances (Biver et al., 1997). This explanation seems unlikely for 19P/Borrelly, owing to the closer distance to Sun. Indeed, outgassing from icy grains, if any, would occur mainly within the inner collisional coma. Molecules released in the collisional coma acquire the bulk average expansion velocity of the gas outflowing from the nucleus through conversion of translational energy. Furthermore, contemporaneous observations of HCN and OH radio lines exist for a number of comets near 1 AU from the Sun. No significant differences between the HCN and OH velocity shifts were ever observed. A good example is again 109P/Swift–Tuttle. Its OH lines show strong blueshifts (Bockelée-Morvan et al., 1994a), which are remarkably similar to those observed for the HCN lines (Bockelée-Morvan et al., 1994b; Despois et al., 1996), once the Greenstein effect has been taken into account.

The map of the H_2O brightness distribution (Fig. 4) is of little help in discriminating between the two alternatives. Indeed, the position angles of the α-jet and comet–Sun directions differed by a few degrees only in September 22–24, 2001 (PA of 94 and 101°, respectively). The variation of the H_2O 557 GHz brightness with (RA, Dec) offset suggests increased H_2O column density towards the East (Fig. 4), in agreement with preferential water outgassing along the α-jet or towards the Sun. CN and C_2 radial profiles along the comet–Sun line show similar sunward/tailward asymmetry (Farnham and Cochran, 2002). It would have been interesting to compute the H_2O brightness distribution in the two alternatives, that is with the density distributions (2) and (3) fitting the HCN line shapes. Significant differences would have been seen as the production rate within the jet is much higher in case (3) than in case (2). However, no H_2O radiative transfer model dealing with an asymmetric coma has

been developed so far, and such a calculation is beyond the scope of the present paper. In addition, the individual H_2O spectra on the map have low signal-to-noise ratios, so that it is questionable whether this would have led to a conclusive result anyway.

In summary, the analysis of the HCN and OH line shapes would favor preferential outgassing towards the Sun rather than outgassing towards the α-jet direction. DS1 images showed a fan-shaped structure centered on the comet–Sun line, second in brightness only to the main α-jet (Soderblom et al., 2002), which could be the dust counterpart of this gas distribution. On the other hand, this solution is not consistent with the analysis of the water production curve made by Schleicher et al. (2003), which argues for a source region at the base of the α-jet. Progress on this question requires detailed gas-dynamics modelling of 19P/Borrelly's coma (e.g., Crifo and Rodionov, 1999).

5. Summary

We have reported radio molecular observations of Comet 19P/Borrelly performed at its 1994 and 2001 apparitions. These observations were intended to investigate compositional differences between Jupiter-family and Oort cloud comets and to provide information on the outgassing of this comet at the time of the Deep Space 1 encounter. The following results were obtained:

- no significant variations in the OH production rate are seen pre-perihelion ($r_h = 1.37$–1.48 AU) between the two passages. This is consistent with results obtained by OH narrowband photometry;
- the HCN production rate at $r_h = 1.36$ AU post-perihelion was significantly smaller in 2001 than in 1994, while similar H_2O and CN production rates are reported for contemporaneous periods. However, similar HCN production rates can be obtained for 1994 and 2001 if the HCN distribution was strongly anisotropic and directed towards the α-jet seen on visible images of the dust coma;
- the H_2O 557 GHz line was detected with the Odin satellite at the time of the DS1 flyby. The line is redshifted with respect to the HCN line, and this displacement is mainly due to self-absorption effects in the water optically thick line;
- the HCN and OH line shapes are asymmetric and blueshifted. Similar Doppler shifts are observed for 1994 and 2001. Since the geometrical conditions were almost identical at the two apparitions, this suggests a similar outgassing pattern of the nucleus in 1994 and 2001, as observed for the dust coma;
- the modelling of HCN line shapes and comparison between OH and HCN velocity offsets favor preferential outgassing towards the Sun, which could be associated with the bright fan-shaped dust structure seen on DS1 images. A dominant outgassing towards the α-jet direction can fit the HCN data, assuming that most molecules are confined within a limited angular extent and that their expansion velocity is unrealistically high compared to measurements made in other comets. This solution is the one proposed by Schleicher et al. (2003) to explain the strong seasonal effects in the observed gas production curves. Following these authors, Farnham and Cochran (2002) modelled the non-gravitational forces and constrained the mass and density of the nucleus of 19P/Borrelly. Further work on this issue must take into account the net velocity of the whole HCN coma inferred by radio measurements;
- due to the moderate activity of 19P/Borrelly, the detection at millimeter wavelengths of molecules other than OH, H_2O, and HCN was not easy. Only marginal detections were obtained for CH_3OH, H_2CO, and CS, while these species have been detected in a number of Oort cloud comets. It is unfortunate that none of these species have been detected in 19P/Borrelly at both 1994 and 2001 apparitions, as this might have helped to resolve the conflict between the HCN and H_2O production rates quoted above, which affects the abundance determinations.

Our knowledge of the molecular composition and outgassing of Comet 19P/Borrelly will certainly benefit from further observations in the radio domain at future apparitions.

Acknowledgments

We are very grateful to Brian Marsden and Daniel Green (CBAT) for providing us updated orbital elements of the comet before the observations. Thanks to David Schleicher for estimating the effect of solar activity on the OH and CN production rates derived from narrowband photometry. Odin is a Swedish-led satellite project funded jointly by the Swedish National Space Board (SNSB), the Canadian Space Agency (CSA), the National Technology Agency of Finland (Tekes), and the Centre national d'études spatiales (CNES, France). The Swedish Space Corporation is the prime contractor, also responsible for Odin operations. The Nançay Radio Observatory is the Unité scientifique de Nançay of the Observatoire de Paris, associated as Unité de service et de recherche (USR) No. B704 to the French Centre national de la recherche scientifique (CNRS). The Nançay Observatory also gratefully acknowledges the financial support of the Conseil régional of the Région Centre in France. This work was supported by the Programme national de planétologie of Institut national des sciences de l'univers et de l'environnement (INSUE).

References

A'Hearn, M.F., Millis, R.L., Schleicher, D.G., Osip, D.J., Birch, P.V., 1995. The ensemble properties of comets: results from narrowband photometry of 85 comets, 1976–1992. Icarus 118, 223–270.

Biver, N., 1997. Molécules mères cométaires: observations et modélisations. PhD thesis. Université de Paris 7.

Biver, N., Bockelée-Morvan, D., Colom, P., Crovisier, J., Davies, J.K., Dent, W.R.F., Despois, D., Gérard, E., Lellouch, E., Rauer, H., Moreno, R., Paubert, G., 1997. Evolution of the outgassing of Comet Hale–Bopp (C/1995 O1) from radio observations. Science 275, 1915–1918.

Biver, N., Bockelée-Morvan, D., Crovisier, J., Davies, J.K., Matthews, H.E., Wink, J.E., Rauer, H., Colom, P., Dent, W.R.F., Despois, D., Moreno, R., Paubert, G., Jewitt, D., Senay, M., 1999a. Spectroscopic monitoring of Comet C/1996 B2 (Hyakutake) with the JCMT and IRAM radio telescopes. Astron. J. 118, 1850–1872.

Biver, N., Bockelée-Morvan, D., Colom, P., Crovisier, J., Germain, B., Lellouch, E., Davies, J.K., Dent, W.R.F., Moreno, R., Paubert, G., Wink, J., Despois, D., Lis, D.C., Mehringer, D., Benford, D., Gardner, M., Phillips, T.G., Gunnarsson, M., Rickman, H., Winnberg, A., Bergman, P., Johansson, L.E.B., Rauer, H., 1999b. Long-term evolution of the outgassing of Comet Hale–Bopp from radio observations. Earth Moon Planets 78, 5–11.

Biver, N., Crovisier, J., Davies, J.K., Despois, D., Lis, D.C., Bockelée-Morvan, D., Colom, P., Gérard, E., Matthews, H.E., Paubert, G., 1999c. Coordinated radio observations of Comet 21P/Giacobini–Zinner in October–November 1998. In: Abstracts Book for Asteroids, Comets, Meteors Meeting, 26–30 July 1999. Cornell University, Ithaca.

Biver, N., Bockelée-Morvan, D., Crovisier, J., Henry, F., Davies, J.K., Matthews, H.E., Colom, P., Gérard, E., Lis, D.C., Phillips, T.G., Rantakyrö, F., Haikala, L., Weaver, H.A., 2000. Spectroscopic observations of Comet C/1999 H1 (Lee) with the SEST, JCMT, CSO, IRAM, and Nançay radio telescopes. Astron. J. 120, 1554–1570.

Biver, N., Bockelée-Morvan, D., Crovisier, J., Colom, P., Henry, F., Moreno, R., Paubert, G., Despois, D., Lis, D.C., 2002. Chemical composition diversity among 24 comets observed at radio wavelengths. Earth Moon Planets 90, 323–333.

Bockelée-Morvan, D., 1987. A model for the excitation of water in comets. Astron. Astrophys. 181, 169–181.

Bockelée-Morvan, D., Crovisier, J., 1985. Possible parents for the cometary CN radical—photochemistry and excitation conditions. Astron. Astrophys. 151, 90–100.

Bockelée-Morvan, D., Bourgois, G., Colom, P., Crovisier, J., Gérard, E., Jorda, L., 1994a. Observations of OH in P/Swift–Tuttle and in several recent weak comets with the Nançay radio telescope. Planet. Space Sci. 42, 193–198.

Bockelée-Morvan, D., Padman, R., Davies, J.K., Crovisier, J., 1994b. Observations of submillimetre lines of CH_3OH, HCN, and H_2CO in Comet P/Swift–Tuttle with the James Clerk Maxwell Telescope. Planet. Space Sci. 42, 662–665.

Bockelée-Morvan, D., Biver, N., Colom, P., Crovisier, J., Gérard, E., Jorda, L., Davies, J.K., Dent, W.R.F., Colas, F., Despois, D., Paubert, G., Lamy, P., 1995. Visible and radio observations of Comet 19 P/Borrelly. Bull. Am. Astron. Soc. 27, 1144.

Bockelée-Morvan, D., Lis, D.C., Wink, J.E., Despois, D., Crovisier, J., Bachiller, R., Benford, D.J., Biver, N., Colom, P., Davies, J.K., Gérard, E., Germain, B., Houde, M., Mehringer, D., Moreno, R., Paubert, G., Phillips, T.G., Rauer, H., 2000. New molecules found in Comet C/1995 O1 (Hale–Bopp). Investigating the link between cometary and interstellar material. Astron. Astrophys. 353, 1101–1114.

Bockelée-Morvan, D., Biver, N., Colom, P., Crovisier, J., Festou, M.C., Henry, F., Lecacheux, A., Weaver, H.A., 2002. Radio investigations of 19P/Borrelly in support to the Deep Space 1 flyby. Earth Moon Planets 90, 459–461.

Chiu, K., Neufeld, D.A., Bergin, E.A., Melnick, G.J., Patten, B.M., Wang, Z., Bockelée-Morvan, D., 2001. Post-perihelion SWAS observations of water vapor in the coma of Comet C/1999 H1 (Lee). Icarus 154, 345–349.

Cochran, A.L., Barker, E.S., 1999. McDonald observatory spectral observations of Comet 19P/Borrelly. Icarus 141, 307–315.

Combi, M.R., Delsemme, A.H., 1980. Neutral cometary atmospheres. I. An average random walk model for photodissociation in comets. Astrophys. J. 237, 633–640.

Crifo, J.-F., Rodionov, A.V., 1999. Modelling the circumnuclear coma of comets: objectives, methods and recent results. Planet. Space Sci. 47, 797–826.

Crovisier, J., 1989. The photodissociation of water in cometary atmospheres. Astron. Astrophys. 213, 459–464.

Crovisier, J., Colom, P., Gérard, E., Bockelée-Morvan, D., Bourgois, G., 2002a. Observations at Nançay of the OH 18-cm lines in comets. The data base. Observations made from 1982 to 1999. Astron. Astrophys. 393, 1053–1064.

Crovisier, J., Colom, P., Gérard, E., Bockelée-Morvan, D., Henry, F., Lecacheux, A., Biver, N., 2002b. Observations of the OH 18-cm lines of comets with the recently upgraded Nançay radio telescope. In: Asteroids, Comets, Meteors (ACM 2002). In: ESA SP, Vol. 500, pp. 685–688.

Despois, D., Gérard, E., Crovisier, J., Kazes, I., 1981. The OH radical in comets—observation and analysis of the hyperfine microwave transitions at 1667 MHz and 1665 MHz. Astron. Astrophys. 99, 320–340.

Despois, D., Biver, N., Bockelée-Morvan, D., Colom, P., Crovisier, J., Paubert, G., 1996. Radio line observations of Comet 109P/Swift–Tuttle at IRAM. Planet. Space Sci. 44, 529–539.

Farnham, T.L., Cochran, A.L., 2002. A McDonald observatory study of Comet 19P/Borrelly: placing the Deep Space 1 observations into a broader context. Icarus 160, 398–418.

Festou, M.C., Barale, O., Davidge, T., Stern, S.A., Tozzi, G.P., Womack, M., Zucconi, J.M., 1998. Tentative identification of the parent of CN radicals in comets: $= C_2N_2$. Bull. Am. Astron. Soc. 30, 1089.

Frisk, U., Hagström, M., Ala-Laurinaho, J., Andersson, S., Berges, J.-C., Chabaud, J.-P., Dahlgren, M., Emrich, A., Florén, H.-G., Florin, G., Fredrixon, M., Gaier, T., Haas, R., Hirvonen, T., Hjalmarson, Å., Jakobsson, B., Jukkala, P., Kildal, P.S., Kollberg, E., Lassing, J., Lecacheux, A., Lehikoinen, P., Lehto, A., Mallat, J., Marty, C., Michet, D., Narbonne, J., Nexon, M., Olberg, M., Olofsson, A.O.H., Olofsson, G., Origné, A., Petersson, M., Piironen, P., Pons, R., Pouliquen, D., Ristorcelli, I., Rosolen, C., Rouaix, G., Räisänen, A.V., Serra, G., Sjöberg, F., Stenmark, L., Torchinsky, S., Tuovinen, J., Ullberg, C., Vinterhav, E., Wadefalk, N., Zirath, H., Zimmermann, P., Zimmermann, R., 2003. The Odin satellite. I. Radiometer design and test. Astron. Astrophys. 402, 24–27.

Hamane, T., Kawakita, H., Kinugasa, K., Yamamuro, T., Takeyama, N., 2002. Abundances in Comet 19P/Borrelly at the time of the spacecraft encounters. Publ. Astron. Soc. Japan 54, L35–L37.

Jorda, L., Colas, F., Lecacheux, J., 1994. The dust jets of Comet P/Swift–Tuttle 1992 XXVIII. Planet. Space Sci. 42, 699–704.

Lamy, P.L., Toth, I., Weaver, H.A., 1998. Hubble Space Telescope observations of the nucleus and inner coma of Comet 19P/1904 Y2 (Borrelly). Astron. Astrophys. 337, 945–954.

Lecacheux, A., 2001. Comet C/2001 A2 (LINEAR). IAU Circ., 7706.

Lecacheux, A., Biver, N., 2002. Comet C/2002 C1 (Ikeya–Zhang). IAU Circ., 7910.

Lecacheux, A., Biver, N., Crovisier, J., Bockelée-Morvan, D., Baron, P., Booth, R.S., Encrenaz, P., Florén, H.-G., Frisk, U., Hjalmarson, Å., Kwok, S., Mattila, K., Nordh, L., Olberg, M., Olofsson, A.O.H., Rickman, H., Sandqvist, A., von Schéele, F., Serra, G., Torchinsky, S., Volk, K., Winnberg, A., 2003. Observations of water in comets with Odin. Astron. Astrophys. 402, 55–58.

Mumma, M.J., DiSanti, M.A., Dello Russo, N., Magee-Sauer, K., Rettig, T.W., 2000. Detection of CO and ethane in Comet 21P/Giacobini–Zinner: evidence for variable chemistry in the outer solar nebula. Astrophys. J. 531, L155–L159.

Mumma, M.J., DiSanti, M.A., Dello Russo, N., Magee-Sauer, K., Gibb, E., Novak, R., 2002. The organic volatile composition of Oort cloud comets: evidence for chemical diversity in the giant-planets nebular region. In: Asteroids, Comets, Meteors (ACM 2002). In: ESA SP, Vol. 500, pp. 753–762.

Neufeld, D.A., Stauffer, J.R., Bergin, E.A., Kleiner, S.C., Patten, B.M., Wang, Z., Ashby, M.L.N., Chin, G., Erickson, N.R., Goldsmith, P.F., Harwit, M., Howe, J.E., Koch, D.G., Plume, R., Schieder, R., Snell, R.L., Tolls, V., Winnewisser, G., Zhang, Y.F., Melnick, G.J., 2000. Submillimeter Wave Astronomy Satellite observations of water vapor toward Comet C/1999 H1 (Lee). Astrophys. J. 539, L151–L154.

Oberst, J., Mottola, S., di Martino, M., Hicks, M., Buratti, B., Soderblom, L., Thomas, N., 2001. A model for rotation and shape of Asteroid 9969 Braille from ground-based observations and images obtained during the Deep Space 1 (DS1) flyby. Icarus 153, 16–23.

Samarasinha, N.H., Muller, B.E.A., 2002. Spin axis direction of Comet 19P/Borrelly based on observations from 2000 and 2001. Earth Moon Planets 90, 473–482.

Schleicher, D.G., A'Hearn, M.F., 1988. The fluorescence of cometary OH. Astrophys. J. 331, 1058–1077.

Schleicher, D., Woodney, L.M., Millis, R.L., 2003. Comet 19P/Borrelly at multiples apparitions: seasonal variations in gas productions and dust morphology. Icarus 162, 415–442.

Soderblom, L.A., Becker, T.L., Bennett, G., Boice, D.C., Britt, D.T., Brown, R.H., Buratti, B.J., Isbell, C., Giese, B., Hare, T., Hicks, M.D., Howington-Kraus, E., Kirk, R.L., Lee, M., Nelson, R.M., Oberst, J., Owen, T.C., Rayman, M.D., Sandel, B.R., Stern, S.A., Thomas, N., Yelle, R.V., 2002. Observations of Comet 19P/Borrelly by the miniature integrated camera and spectrometer aboard Deep Space 1. Science 296, 1087–1091.

Weaver, H.A., Feldman, P.D., McPhate, J.B., A'Hearn, M.F., Arpigny, C., Smith, T.E., 1994. Detection of CO Cameron band emission in Comet P/Hartley 2 (1991 XV) with the Hubble Space Telescope. Astrophys. J. 422, 374–380.

Weaver, H.A., Chin, G., Bockelée-Morvan, D., Crovisier, J., Brooke, T.Y., Cruikshank, D.P., Geballe, T.R., Kim, S.J., Meier, R., 1999. An infrared investigation of volatiles in Comet 21P/Giacobini–Zinner. Icarus 142, 482–497.

Weaver, H.A., Stern, S.A., Parker, J.W., 2003. HST/STIS observations of Comet 19P/Borrelly during the Deep Space 1 encounter. Astron. J. 126, 444–451.